IFAC Publications
www.elsevier.com/locate/ifac

ACTUATOR SIMULATION OF THE DAMADICS BENCHMARK ACTUATOR SYSTEM

Michal Bartyś[♣] and Salvador de las Heras[♠]

[♣]*Warsaw University of Technology, Poland, {bartys@mchtr.pw.edu.pl}*
[♠]*Universitat Politècnica de Catalunya, Spain, {delasheras@mf.upc.es}*

Abstract: In the paper the simulation model of actuator consisting of spring-diaphragm pneumatic servomotor, intelligent positioner and control valve is presented. The model is particularly suited to compare and contrast a wide range of fault detection and isolation methods within a strongly oriented focus on application to industrial actuator examples. Using the model it is possible to simulate up to 19 incipient or abrupt faults of the actuator. The model is based on physical description and partly on engineering expertise. The parameters of the model were determined experimentally. Model was validated by application of real process data. *Copyright © 2003 IFAC*

Keywords: actuators, fault detection, fault isolation, modelling, positioning systems, diagnosis, control valves.

1. INTRODUCTION

In the recent years there were developed a number of fault detection and isolation methods of industrial processes. The problem of actuator diagnostics was also considered. Various approaches were developed for actuators' fault detection and isolation:

- parity equation
- unknown input observer
- extended Kalman filter
- signal analysis
- fuzzy logic and neural-fuzzy networks
- b-spline
- information theory

When considering the industrial implementations arise the problem of the assessment of applicability features of FDI methods for actuators. A new industrial application oriented benchmark (Syfert *et al.*, 2002) may be applied to solve this problem. This benchmark may be used either for testing, evaluation or ranking of FDI methods. The set of numerical quantifiers generated by the benchmark utilities is very helpful in this case. The benchmark is build around the actuator reference model. This model is based on analytical description and in part on engineering knowledge of real industrial actuator. Model was tuned and validated applying data originating from real industry process. The novelty of the model lays on the possibility of simulating up to 19 incipient or abrupt faults of the actuator. This paper brings more details about the developed actuator model.

2. ACTUATOR

The modelled device belongs to the class of a electro-pneumatic actuators (Fig. 1.) Actuator or final control element is a physical device, structure or assembly of devices acting on controlled process. We will further understand the actuator as an assembly consisting of:

- control valve
- spring-and-diaphragm pneumatic servomotor
- positioner

Control valve acts on the flow of the fluid passing through the pipeline installation. A servomotor accomplishes changing the position of the control valve plug thus acting indirectly on fluid flow rate. A spring-and-diaphragm pneumatic servomotor is a compressible fluid powered device in which the fluid acts upon the flexible diaphragm, to provide linear motion of the servomotor stem. In industrial practice servomotor is sometimes called as actuator. According to above given definition we will understand the term actuator in more broad sense.
Positioner is a device applied to eliminate the control-valve-stem miss-positions produced by the external or internal sources such as friction, supply pressure instabilities, hydrodynamic forces etc.

Fig.1. Example of final control element (actuator) consisting of: spring-and-diaphragm pneumatic servomotor, positioner and control valve.

3. GENERAL ACTUATOR MODEL

Actuator model was designed basing on general scheme shown on Fig. 2. The actuator's model inputs are: process control value *CV*, pressure on valve inlet *P1*, pressure on valve outlet *P2*, medium temperature *T1* and faults *f*. The actuator's model outputs are: medium flow rate *F* and displacement of valve plug *X*. The model inputs and outputs (except of vector *f*) are referring to the set of potentially available signals from industrial SCADA or DCS systems.

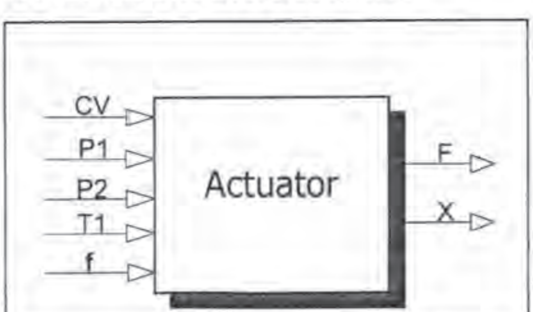

Fig. 2. The general block scheme of actuator.
Notations:

CV	- process control value
P1, P2	- pressures on valve: inlet and outlet
T1	- medium temperature
f	- vector of faults,
F	- flow rate
X	- valve plug displacement

Not all the signals are really available in particular industrial cases. This is however not a reason for limited model applicability. The model was primary designed only for testing the applicability features of fault detection and isolation algorithms. Therefore all the inputs are assumed as available (including vector of faults **f**).

4. THE SET OF ACTUATOR FAULTS

Actuator faults may be either internal: e.g. in control valve, servo-motor, positioner or external e.g. in supply lines. Proper fault isolation has a crucial meaning in practice. For example, the time-to-repair ratio is approximately one order higher depending if the fault is localised in control valve rather than in positioner. The set of actuator faults was given by Kościelny & Bartyś, (2000). This set consists of four classes and 19 faults $\{f_1 .. f_{19}\}$. This set of faults was assumed as a reference one.

The faults are classified into following classes:

- Control valve faults $\{f_1 .. f_7\}$
- Pneumatic servomotor faults $\{f_8 .. f_{11}\}$
- Positioner faults $\{f_{12} .. f_{14}\}$
- General faults/external faults $\{f_{15} .. f_{19}\}$

5. MODEL STRUCTURE

The actuator model consists of three main functional blocks reflecting its physical structure (Fig. 3). The model was based on analytical description of physical behaviour of the actuator (mechanics, fluidics, and thermodynamics). Some simplifications in analytical description were done in order to achieve the compromise between model complexity and model functionality. The admissibility of the assumed simplifications was experimentally verified. The actuator model was also experimentally tuned and validated by making usage of real industrial process data. The appropriate industrial set-up was assembled for this purpose. The experimental set-up was equipped with smart positioner, spring-and-diaphragm pneumatic servomotor, equal percentage control valve and appropriate instrumentation.

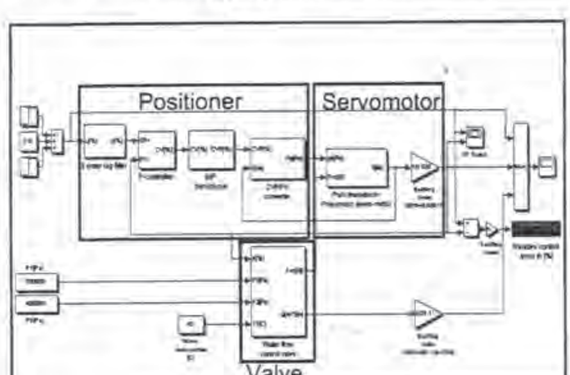

Fig. 3. Actuator model structure.

6. MODEL STRUCTURE

6.1. Positioner

The simplified structure of the positioner model is shown on Fig. 4 and its Matlab-simulink model on Fig.5. Model consists of four main blocks: low-pass filter, P-controller, electro-pneumatic transducer and feedback system. The positioner is used as the follow-up control system of the pneumatic servomotor stem displacement. The input signal (CV) of the positioner is fed from the external controller. The pressure signal *Ps* is the output signal of positioner. This pressure is supplying the chamber of pneumatic servomotor. Internal feedback signal x is used as a process value signal for proportional controller of positioner.

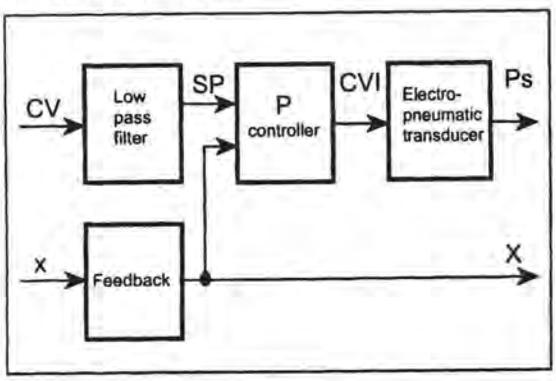

Fig. 4. Positioner model structure.

Four faults are considered in positioner: the electro-pneumatic transducer fault, stem displacement sensor fault, positioner mechanical feedback fault and positioner pressure sensor fault (Bartyś and Syfert, 2002). The individual fault development scenarios are assigned to each fault. In Tab. 1 the description of simulation method of positioner fault *f13* is given for example. Because the actuator model is not a "black box model", the faults have his own "entries" into the model. These entries are shown for example on Fig.6. Additionally standardised fault strength attribute has been assigned to each fault. Interpretation of fault strength is fault nature dependent.

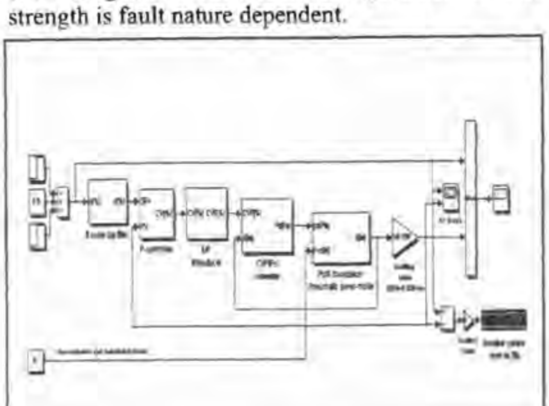

Fig. 5. Matlab simulink positioner model structure

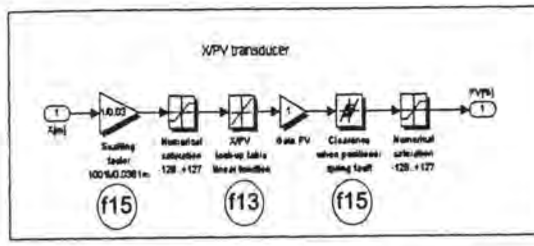

Fig. 6. Positioner feedback fault entries. Notations:
f_{13} – servomotor's stem displacement sensor fault
f_{15} – spring fault in mechanical feedback system

Table 1. Simulation technique of fault f13

Fault	f13
Group	Positioner
Description	stem displacement sensor fault
Physical interpretation	wear of the potentiometer conductive plastic layer or wear or fatigue of potentiometer wiper or wiring break or displacement electronics failure
Fault primary nature	slowly developing
Simulated action	simulated as a change of stem displacement measurement
Fault strength limits	{-1..1}
Fault strength interpretation	-1 relative stem displacement = 0 0 no fault; 1 relative stem displacement = 1
Fault simulation technique equation	$X_f = X_0(1+1.25f_s)$ X_f – *relative displacement measurement* X_0 – *relative stem displacement* f_s – *fault strength*

6.2. Spring-diaphragm pneumatic servomotor

The servomotor converts the pneumatic pressure into the linear mechanical displacement of the stem. The simplified servomotor scheme is given on Fig. 7. Fig. 9 shows the scheme of forces acting on servomotor's stem.

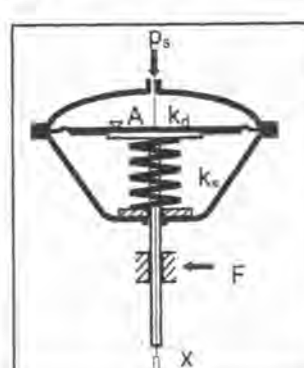

Fig.7. Scheme of pneumatic spring-diaphragm servomotor.

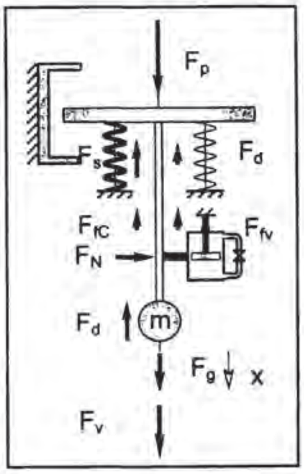

Fig.8. Dynamic force equilibrium scheme in pneumatic servomotor.

Servomotor stem movement model

Servo-motor's stem movement description is derived from:

$$m\ddot{x} + k_v\dot{x} + sign\,(\dot{x})F_N\mu + (k_s + k_d)x + \quad (1)$$

$$- F_{vc}(x) + (k_s + k_d)x_0 - mg = p_s A_e$$

where:

F_p - diaphragm active force
F_s - spring force
F_p $= p_s A_e$
F_s $= k_s(x + x_0)$
F_d $= k_d(x + x_0)$
F_{fC} $= \mathrm{sgn}(\dot{x})F_N\mu$
F_{fv} $= k_v\dot{x}$
F_{dA} $= m\ddot{x}$
F_{vc} $= f(x, P1, P2, F, Kv, \rho)$
k_s - spring constant
x - stem displacement
x_o - initial spring deflection
F_d - spring deflection force
k_d - diaphragm spring constant
F_{fC} - Coulomb friction force
F_{fv} - viscous friction force
F_{dA} - d'Alembert force
F_{vc} - reaction force of valve plug
m - combined mass of moving parts
μ - friction constant
A_e - effective diaphragm area
ρ - fluid specific gravity
F - volume flow rate
K_v - liquid sizing coefficient

Model of pneumatic chamber

The conversion of internal gas energy into mechanical one takes place in the pneumatic chamber of servomotor. Considering that gas compressibility can not be neglected and assuming gas flow continuity, the mass volume rate may be given by:

$$\dot{m}_g = \rho\dot{V} + V\dot{\rho} \quad (2)$$

The hypothesis of local thermodynamic gas equilibrium may be considered in the phase of chamber unloading *($dm_g/dt<0$)*. This hypothesis is principally not valid in the case of chamber loading, except of small volume chamber, in which assumption of homogenous pressure distribution is admissible. The hypothesis of polytropic gas transformation in a chamber (Sorli *et al.*, 1999) is to be considered when assuming that heat energy is not exchanged with the environment and the external parameters (supply air pressure, temperature) are constant. Other, more advanced models (Kagawa & Ohligschläger, 1990) are taking into consideration the heat exchange with environment and thermal evolution of energy conversion. These models are impracticable because of necessity of identifying too many model parameters. Scavarda and Richard (1994) stated the acceptability of isothermal gas transformation for pneumatic drives. The classical polytropic equation has a form:

$$\frac{p_1}{\rho_1^\kappa} = \frac{p_2}{\rho_2^\kappa} \quad (3)$$

where appropriate lower and upper indices are related to the gas states in the time moments differing by value of Δt. If the polytropic exponent κ is constant in the time interval Δt then after differentiation of (3):

$$\kappa = \frac{\dot{p}/p}{\dot{\rho}/\rho} \quad (4)$$

After substitution of $\dot{\rho}$ to the gas continuity equation (2) we obtain gas accumulation equation with the capacity parameter depending on the gas state.

$$\dot{p} = \frac{1}{\left[\frac{\kappa p}{\rho V}\right]}(\dot{m} - \rho\dot{V}) \quad (5)$$

Assuming isothermal gas transformation during chamber loading and unloading i.e. after acceptance of $\kappa=1$, the equation (5) will have a form:

$$p = \frac{1}{\left[\frac{RT_0}{V}\right]}\int_0^t (\dot{m} - \rho\dot{V})dt \quad (6)$$

The actuator model assumes isothermal air transformation in servomotor chamber. The simulated processes of loading and unloading of servomotor chamber is shown on Fig. 9.

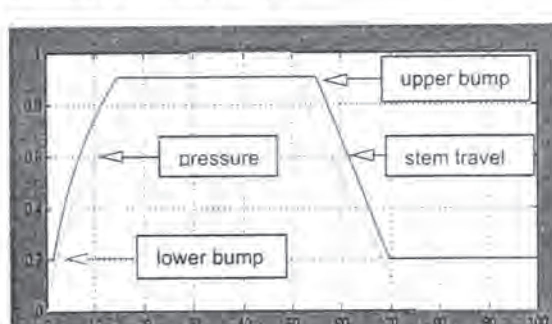

Fig. 9. Simulation results of loading and unloading of servomotor chamber.

Model of friction

Packing friction opposes valve stem movement in any direction. Friction is strongly dependent upon packing material applied. The friction force shares up to 20% of total active force developed by servomotor (Fig. 10). Characteristic feature of friction is its non-continuity in region of travel velocities close to zero. The friction force is balancing external forces in the phase of stickiness until the Coulomb force will overcome. In the microscopic scale the stickiness cause microscopic plastic material deformations thus dissipating energy. In the stickiness phase the friction force should be rather considered as a function of position and not velocity (Haessig and Friedland, 1991). In the slip phase the friction forces are depending on the shape and material of packing, lubricants used, surface roughness e.t.c. For simulation purposes the classical description of friction phenomenon given by Karnopp (1985) was implemented. In this model the friction force is equal to the sum of all external forces in the stickiness phase. Influencing on friction parameters gives in this case the opportunity of simulation of twisty servomotor's stem fault (Tab. 2) or effects of packing wear, stem corrosion e.t.c.

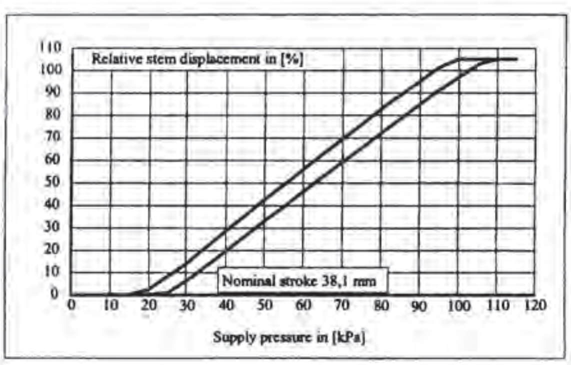

Fig.10. Experimental results of relative stem displacement versus servomotor supply pressure of reverse-acting pneumatic-diaphragm servomotor. Hysteresis loop results mainly from the packing friction.

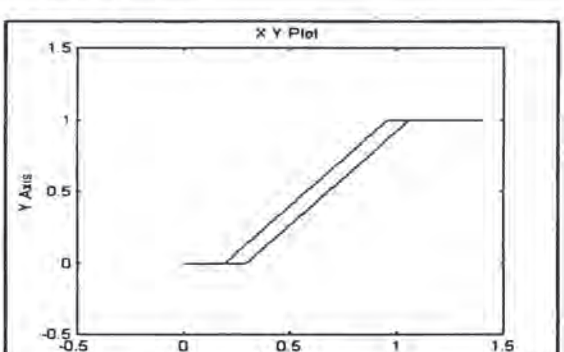

Fig. 11. An example of simulated relative stem displacement versus servomotor supply pressure.

Tab. 2. Fault f8 simulation technique

Fault	f8
Group	pneumatic servomotor
Description	twisted servomotor's stem
Physical interpretation	permanent bending of the servomotor's stem due to mechanical tensions caused by the internal or external forces acting on stem perpendicular to its axis
Fault nature	abrupt
Simulated action	simulated as a linear change of friction hysteresis loop width versus stem displacement
Fault strength limits	{0..1}
Fault strength interpretation	0 – no twist; 1- advanced twist
Fault simulation technique equation	$D_{hf} = \min\{P_{t0}, \max[0, D_h(1+0.5*f_s(1-X))]\}$ D_{hf} – *hysteresis loop width in [m]* D_h – *input hysteresis loop in [m]* P_{t0} – *nominal plug travel (0.0381 m)* f_s – *fault strength* X – *relative stem displacement*

Model of control valve

For the simulation of the liquid flow, the Bernoulli's continuous flow law for incompressible, inviscid fluids in following engineering form was applied:

$$F = 0{,}1K_v\sqrt{\frac{\Delta p}{\rho}} \tag{7}$$

F - flow rate
Δp - fluid pressure drop across the valve
ρ - liquid specific gravity in upstream [kg/ m^3]
K_v - liquid sizing coefficient

The inherent valve flow characteristics is strongly dependent on valve geometry. Therefore liquid sizing coefficient K_v is a function on the valve opening X. In the actuator model the valve flow characteristics may be easy changed by modification of the normalised function $K_v(X)$. However for benchmark purposes the equal percentage flow characteristics was fixed.

Cavity phenomenon

The cross-section area of control valves varies in a wide range during normal operation. Therefore the cavity phenomena conditions may be satisfied if fluid outlet pressure *P2* recovers to a pressure above the vapour pressure of the liquid. Intensive cavitation drastically shortens the operating life time of the installation. If the fluid outlet pressure *P2* remains below the vapour pressure of the liquid, flashing effect occurs. If the cavitation occurs, the flow law (7) is not more valid. The bi-phase flow depends in

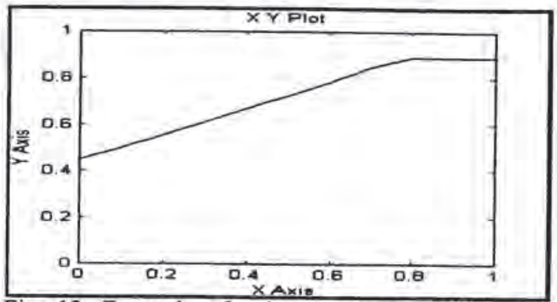

Fig. 12. Example of valve recovery coefficient K_m versus valve opening X for a typical global valve.

this case from the pressure difference between liquid upstream $P1$ and vapour pressure p_v of the liquid. If the liquid temperature is constant the flow is theoretically dependent only from the pressure $P1$. In fact valve design influence on this flow in practice (Coughran, 1996). Therefore valve manufacturers are defining additional engineering factors such as for example: valve recovery coefficient K_m and critical pressure ratio of the liquid r_c. Valve recovery coefficient depends on the valve opening K_m. Critical pressure ratio r_c depends mainly on upstream fluid pressure.

$$F = 0{,}1K_v\sqrt{\frac{\Delta p_{all}}{\rho}} \quad ; \quad \Delta p_{all} = K_m(P1 - r_c p_v) \qquad (8)$$

where:

K_m - valve recovery coefficient

r_c - critical pressure ratio of the liquid

p_v - upstream fluid vapour pressure

The liquid evaporation conditions are tested in actuator model basing on logarithmic pressure-temperature law:

$$\log \ p_v = -\frac{a}{T} + b \qquad (9)$$

where a and b are liquid dependent. The actuator model was tuned assuming water as a controlled medium.

7. MODEL VALIDATION

Actuator model was validated by application of real process data (Bartyś and Syfert, 2002) from the actuator controlling water inflow into power station boiler of sugar factory. An example of validation procedure results is shown on Fig. 13. Maximal value of stem displacement error does not exceed 7.5%. The measurement uncertainty equals 2%.

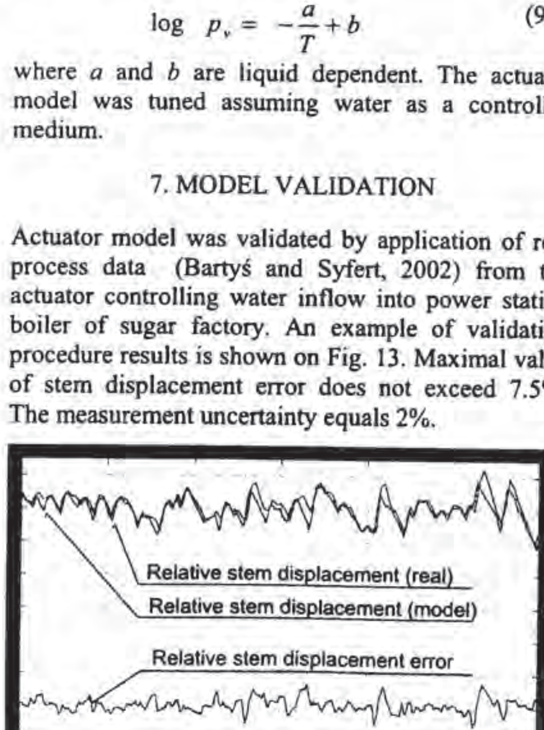

Fig. 13. Example of actuator validation results.

8. SUMMARY

The actuator model intended for FDI methods evaluation prior to industrial implementations was announced. Model was tuned experimentally using process data acquired from real industrial process. Validation of the model was done. Model was implemented in matlab-simulink environment. Model was designed basing on analytical description of physical phenomena combined with engineering knowledge and results of experiments. Model was supplied with 19 fault entries. Every entry was clearly defined. This simplifies its application for investigations of industrial applicability of FDI algorithms.

ACKNOWLEDGEMENTS

The authors acknowledge funding support under the EC RTN contract (RTN-1999-00392) DAMADICS. Thanks are expressed to the management and staff of the Lublin sugar factory in Poland for their collaboration and provision of manpower and access to their sugar plant.

REFERENCES

Bartyś, M., and M. Syfert (2002). Using Damadics Actuator Benchmark Library (DABLib). In: *http://diag.mchtr.pw.edu.pl /damadics/.*

Coughran, M. (1996). Performance influences in globe control valves, *Intech*, Vol. **43**, No. 8,.

Haessig, D.A. and B. Friedland (1991). *On the Modelling and Simulation of Friction*. Transactions of the ASME. Journal of Dynamic Systems, Measurement and Control. 113, pp. 354-362.

Kagawa, T., and O. Ohligschläger (1990). Simulationsmodell für Pneumatische Zylinder-antriebe. *Ölhydraulik und Pneumatik*. No 34. pp. 115-120.

Karnopp, D. (1985). Computer Simulation of Stick-Slip Friction in Mechanical Dynamic Systems, *Transactions of the ASME. Journal of Dynamic Systems, Measurement and Control*. No 107, pp. 100-103.

Scavarda, S., and E. Richard (1994). *Non linear Control of Electropneumatic and Electrohydraulic Servodrives*: A Comparison". 11th Aachener Fluidtechnisches Koloquium. Aachen, pp. 223-236.

Sorli, M., L. Gastaldi, E. Codina and S. de las Heras (1999). *Dynamic Analysis of Pneumatic Actuators*. Simulation Practice and Theory. Special Issue on Bondgraphs for Modeling and Simulation. **7**, pp. 589-602.

Syfert, M., M. Bartyś, J. Quevedo (2002). Benchmark definition. In: *http://diag.mchtr.pw.edu.pl/damadics*

Syfert, M., M. Bartyś, R. J. Patton and J. Quevedo (2003). Development and Application of Methods for Actuator Diagnosis in Industrial Control Systems (DAMADICS): A Benchmark Study, In: proceedings of IFAC Symposium SAFEPROCESS '2003, Washington, USA.